

2015, 44 (116), 155–161
ISSN 1733-8670 (Printed)
ISSN 2392-0378 (Online)
DOI: 10.17402/071

Received: 31.08.2015

Accepted: 20.10.2015

Published: 07.12.2015

Performance of a novel Receiver Autonomous Integrity Monitoring procedure consistent with IMO requirements

Michael Mink¹✉, Bernhard Heck²

¹ Airbus Defence and Space

1 Willy-Messerschmitt-Straße, 85521 Ottobrunn, Germany, e-mail: Michael.Mink@airbus.com

² Karlsruhe Institute of Technology

7 Englerstraße, 76131 Karlsruhe, Germany, e-mail: Bernhard.Heck@kit.edu

✉ corresponding author

Keywords: Global Navigation Satellite Systems, integrity, Receiver Autonomous Integrity Monitoring, maritime, International Maritime Organization, protection level

Abstract

Although integrity concepts for Global Navigation Satellite Systems (GNSS) are ubiquitous in the aviation community, integrity algorithms of comparable maturity have not yet been developed for maritime users. The International Maritime Organization (IMO) specifies requirements different from those specified by the International Civil Aviation Organization (ICAO). These different requirements affect the design of the integrity algorithms with respect to integrity risk allocation and threat space. This paper describes a novel integrity algorithm based on conditions valid for maritime users. The performance of the novel integrity algorithm has been assessed and compared to a conventional Receiver Autonomous Integrity Monitoring (RAIM) approach consistent with IMO requirements.

Introduction

Integrity concepts such as Receiver Autonomous Integrity Monitoring (RAIM) provide integrity autonomously at user level. RAIM was originally developed for the aviation community, and aviation-specific algorithms have attained an advanced state of maturity. However, integrity algorithms designed specifically for maritime users have not reached a comparable maturity level. This paper describes the derivation of a novel integrity algorithm that provides statistical bounds on the position error for maritime users. The fact that maritime users move exclusively along the sea surface, which is approximated by the geoid model, presents the opportunity of using additional height information. Specifically, additional height information derived from the geoid model can be used to perform a cross-check with Global Navigation Satellite Systems (GNSS)-derived height information. In reality, geoid-derived heights do not precisely coincide with the sea surface, because they do not

adequately account for such factors as tides and waves. This paper describes the correction of errors in geoid-based height estimates caused by such factors as tides and waves. However, an assumption about the residual deviation of the sea surface and the geoid height needs to be made. Assuming that heights from the geoid bound the true height with a certain probability allows for a degree of fault detection (FD). This paper evaluates the possibility of performing FD based on a test statistic expressed as the difference between the height derived from the geoid and the height based on GNSS. Furthermore, a scheme is proposed by which the horizontal protection level (HPL) may be derived from this test statistic. The performance of this algorithm is compared to the Least-Squares Residual (LSR) RAIM approach (Sturza, 1988–1989; Brown, 1992; Navipedia, 2014).

The paper is structured as follows. In a first step, the requirements of the International Maritime Organization (IMO) are described. Then the derivation of the reference height from a geoid model is

described, including the kinds of effects that this derivation must consider. The novel algorithm that includes a FD and HPL scheme is presented in theory. A short comparison to the LSR RAIM approach concludes the theoretical description. The paper ends with a comparison of the performance of both RAIM approaches.

IMO performance requirements

This section summarizes IMO requirements for open sea operation. From this, the performance requirements for the RAIM algorithm in terms of the probability of false alert, (P_{fa}), and the probability of missed detection, (P_{md}), are derived. The P_{md} is a function of the allowed integrity risk, whereas the probability of false alert must be set in such a way that the requirement for continuity is satisfied. According to IMO (IMO, 2002), the following requirements will be assumed:

Table 1. IMO Requirements

Operation	Accuracy (h/v)	HAL/VAL	Int. Risk	Cont. Risk
Open Sea	10 m/-	25 m/-	1E-5 /3 h	3E-3 over 3 h

Deriving ellipsoidal height from geoid

The geoid is the shape that the surface of the oceans would take under the influence of Earth's gravity and rotation alone, in the absence of any other influences such as winds and tides. Specifically, the geoid is the equipotential surface that would coincide with the mean ocean surface of the Earth if the oceans and atmosphere were in equilibrium and at rest relative to the rotating Earth. According to Gauss, who first described it, the geoid is the "mathematical figure of the Earth," a smooth but irregular surface that does not correspond to the actual surface of the Earth's crust, but to a surface which can only be known through extensive gravity measurements and calculations. A commonly used geoid model is the EGM08 (EGM08, 2008).

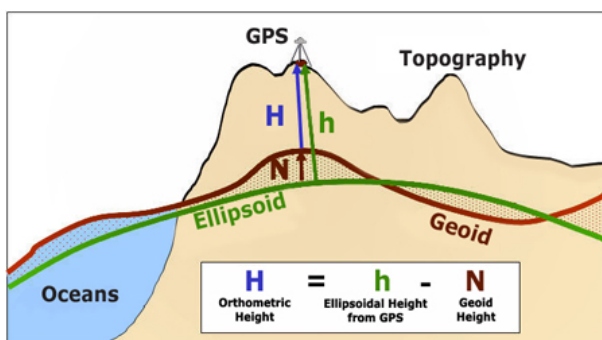


Figure 1. Relation between geoid and ellipsoid

GNSS uses an ellipsoid as a global reference surface. Hence, the geoid at height N is needed to translate ellipsoidal height from the GNSS height, h , to the geoid, and vice versa (Figure 1). As indicated, several factors that cause the ocean's surface to deviate from the geoid must be considered in order to derive an adequate reference height from the geoid. Some major effects are pointed out below along with the respective mitigation actions to reduce their impact on the final height estimation:

- Hydrostatic effects;
- Hydrodynamic effects;
- Geodynamic processes.

The fact that a ship with a certain shape and weight moves on water introduces hydrostatic effects. Trimming describes the rotation about the lateral axis, which comprises separate static and dynamic components. Static trimming depends on load, and its centre of mass, the shape of the ship, and the lifting power of the water. Dynamic trimming is caused by the hydrodynamics of the ship. It is analogous to heeling, which describes the same effects but along the direction of motion. Hydrodynamic effects must also be considered. The diving of a ship into its own wave system is called the "squat effect." The water runs with higher velocity around the ship's body, resulting in a change of water pressure. Hence, increased velocity of the ship is associated with a drop of the ship. Geodynamic processes affect the total ocean surface, and can be structured into high- (waves) and low-frequency (tides) effects. Waves are a function of position and time, and cause vertical movements of the ship. In order to reduce or mitigate the impact on height due to wave motions, a three-axis gyro can be applied to correct position and height of the GNSS antenna for this effect. Ocean tides cause periodic variations of the sea surface due to tidal forces. The time period between tidal high and low water levels is designated as times of low and high tides. The magnitude of the impact can be modelled and mitigated over time.

It needs to be pointed out that at this point the list of effects identified here is neither complete nor discussed in detail. This paper does not focus on a discussion of these effects, but intends to raise an awareness of their presence. Figure 2 gives an overview of the relationship between the different height definitions.

The ellipsoid is the reference surface which the GNSS height, (h_{GNSS}), is referenced to. The ellipsoidal height, ($h_{Ellipsoid}$), can be converted to a geoid height, (h_{Geoid}), by applying the offset N , which is known as the "geoid undulation." N is assumed to

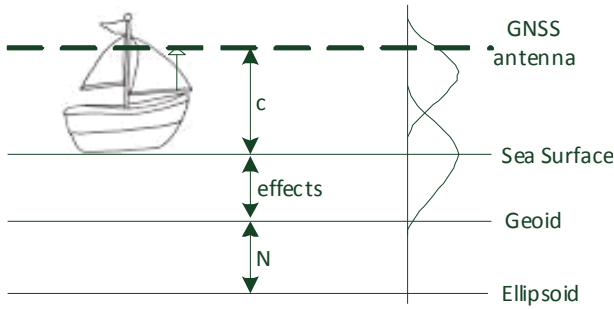


Figure 2. Height definitions

be known and hence error-free, although the accuracy of N at ocean level is typically less than 1 m. In this paper, the true height refers to h_{Geoid} . Under the theoretical conditions described above, the geoid equals the sea surface. However, due to the presence of various effects, this is not precisely the case. The set of factors causing variations between the sea surface, ($h_{\text{sea surface}}$), and the geoid, (h_{Geoid}), will be referred to as the “effects”. In addition, because of the uncertainty associated with these effects, $h_{\text{sea surface}}$ is assumed to have an error distribution. A ship moving along the sea surface with a GNSS antenna on board computes h_{GNSS} . Because the GNSS antenna is mounted somewhere on the ship, a constant offset, c , must be applied to refer to the height of the sea surface precisely. This offset is assumed to be known, and variations due to such factors as the weight of the ship are ignored in this paper.

In summary, we can obtain a height for the sea surface derived from the geoid, and a height derived from GNSS, referenced to the sea surface by the expression ($h_{\text{GNSS}} = h_{\text{GNSS}'} - c$). The next step in the derivation is to account for the error in GNSS measurements if the both estimates for sea surface height are sufficiently different. The threshold above which significant height differences are assumed is denoted TH . The error distribution for h_{GNSS} is assumed to be Gaussian, but not necessarily centralized. True height is assumed to be bounded by $h_{\text{sea surface}}$ with a certain probability. The vertical position error is characterized by the following relationship:

$$\sigma_{\text{ver}} = \sqrt{\sum_{i=1}^n (S_{U,i} \sigma_i)^2} = \sqrt{\sum_{i=1}^n \sigma_{U,i}^2} \quad (1)$$

In Eq. (1), S is the projection matrix to map from range to position domain. The noise of each pseudo range i is denoted by σ_i . Similarly, the position error in the horizontal component is given by the following expression:

$$\sigma_{\text{hor}} = \sqrt{\sum_{i=1}^n S_{\text{hor}} \sigma_i^2} \quad (2)$$

The estimates for position and receiver clock offset are composed as \hat{x} , and computed following the least-squares approach as follows:

$$\hat{x} = (H^T W H)^{-1} H^T W y = S y \quad (3)$$

In Eq. (3), the Jacobian matrix (or Design-Matrix) is denoted H , and the inverse co-variance matrix is denoted W . The vector y contains the pseudo range measurements to each satellite. The matrix S is the projection from the range to the position components (horizontal and up) of the position domain.

Algorithm

This section assesses the fault-detection capability of the algorithm, as well as a derivation of the computations for the horizontal protection level (PL).

Fault detection

True height is derived from the geoid height, (h_{Geoid}). Due to the effects described above, $h_{\text{sea surface}}$ does not equal the true height. Nevertheless, the error distribution of $h_{\text{sea surface}}$ contains the true height with a certain probability. Therefore, the condition that the distribution of $h_{\text{sea surface}}$ does not contain the true height with a given probability might lead to an integrity issue which must be accounted for in the integrity risk allocation. The probability P_1 that the distribution of $h_{\text{sea surface}}$ does not contain the true height is defined as follows:

$$P_1 = \int_{-\infty}^{\text{True height}} \sigma_{h_{\text{sea surface}}} dx \quad (4)$$

Based on $h_{\text{sea surface}}$ and its error distribution, the detection threshold TH is set according to the requirement for P_{fa} . Taking into account the true height and the sea surface, the detection threshold is defined as follows:

$$TH = [k(P_1) + k(P_{fa})] h_{\text{sea surface}} \quad (5)$$

The factor k describes the number of sigmas which are related to a certain probability. A failure is detected if h_{GNSS} exceeds the threshold TH , as shown in Figure 3.

In the case of a fault detection, the following two basic options are identified:

- If $|h_{\text{GNSS}} - h'| > TH$, the set of measurements will be excluded; or
- Faulty measurements are identified and excluded by composing and analysing subsets of measurements (Isshiki, 2008).

It is important to note that, in general practice, requirements exist exclusively for the horizontal component, and faults impacting the vertical com-

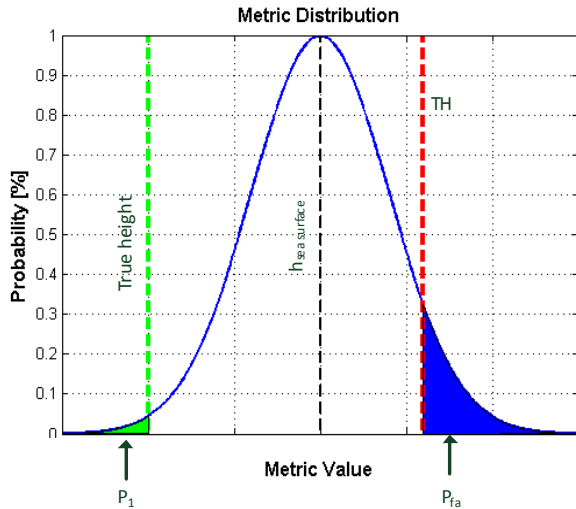


Figure 3. Definition of TH

ponent are not a priority. Therefore, it is important to determine whether faulty measurements detected by their impact on the vertical component also have an impact on the horizontal component. Thus, if a faulty measurement is detected in the vertical component, it must be mapped into the horizontal component to verify its impact. It is clear that ranging errors are only detected for satellites that contribute sufficiently to the vertical component. This means that errors may not be detected if they cannot be detected in the vertical component. Hence, in a first iteration, only satellites whose contribution to the vertical component is greater than the contribution to the horizontal component can be considered for FD. For such satellites I , the following condition is valid:

$$\frac{S_{U,i}}{S_{EN,i}} \geq 1 \quad (6)$$

The preliminary conclusion about the FD capability of the novel integrity algorithm is that the prior condition that must be true is not always given. In order to validate this conclusion, an analysis based on a GPS constellation with 24 satellites has been performed to determine when this condition is met. For each user location at a specific instance in time, the projection matrix reveals the factors for every satellite for projection from the pseudo range domain into the position domain. The analysis considers only the most critical satellite at each user location. The most critical satellite is defined as the satellite whose vertical contribution has the greatest impact on the horizontal position domain, and for which the following condition is met:

$$\min_i \left(\frac{S_{U,i}}{S_{EN,i}} \right) \geq 1 \quad (7)$$

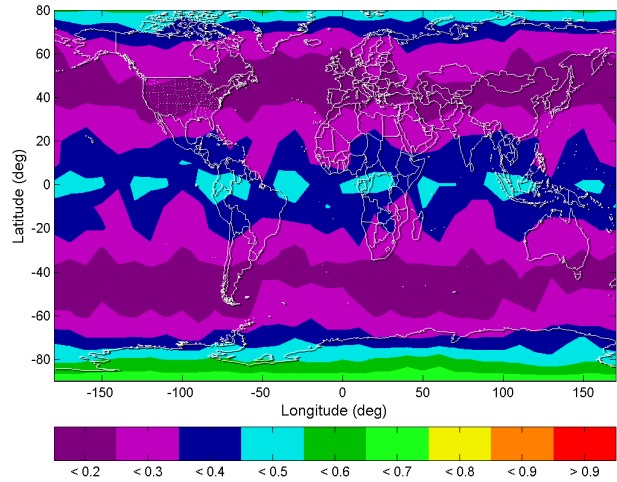


Figure 4. Availability of FD prior condition for GPS only. Masking angle = 25°

The analysis indicated that the mapping factor is strongly dependent on the applied elevation mask. Optimum results can be achieved at an elevation mask of 25°. Results are given in Table 2.

Table 2. Availability of pre-conditions to perform FD

Availability of Pre-condition to perform FD [%]		
Masking angle	25°	10°
GPS only	31.10	5.15

It was concluded that FD capability is dependent on user location. However, averaging the results on a global basis, it was determined that the condition described above is fulfilled ~31% of the time, which means that a FD can be performed during these times. In the absence of any FD mechanisms, the P_{md} would be 1. This means that, in the presence of a failure, no FD can be performed. However, the P_{md} can be tuned according to the results obtained.

Protection level computation

The computation of a horizontal protection level (HPL) is divided into three consecutive steps. The first step identifies the minimum error that can be detected in the vertical component (MDE) based on the requirements for P_{md} and P_{fa} . Then, in the second step, MDE is projected into the horizontal position domain by using the satellite with the minimum contribution to the vertical component. Choosing the satellites whose sensitivity to the vertical component is the lowest ensures that the MDE mapped into the horizontal component bounds the errors in the range domain. In the last step, the HPL is computed.

The minimum detectable error in the vertical component, $MDE_{vertical}$, is defined by the difference of the true height and h , as well as by taking into account the overbounding uncertainty to bound the

mode 2. In the case of a failure mode that the true height is not bounded by $h_{\text{sea surface}}$, this fact causes the position error to exceed the PL .

The failure modes are assumed to be the major instances of service failure because of the wide acceptance regions. According to the GPS signal specification (Global Positioning System, 2008), three major failures per year, assuming 24 satellites, corresponds to an individual major satellite failure with a probability $p \approx 1.43E - 5/h$. The probability of having k simultaneous failures among N satellites in view is:

$$p_{\text{major satellite failure}, N, k} = C_N^k p^k (1 - p)^{N-k} \quad (14)$$

If an average of 8 satellites is in view, the global probability of having a major satellite failure is $\sim 1E - 4/h(P_{\text{occ}})$.

Comparison to LSR RAIM

Comparing the novel RAIM approach presented in this paper to the LSR RAIM, it is obvious that the approaches work in different detection domains. The detection statistic of the LSR RAIM approach is the scalar product of the pseudo range residuals, while the novel RAIM performs FD in the vertical component. This yields limited FD capabilities for the novel maritime RAIM approach, because only faults contributing sufficiently to the vertical component can be detected. Both approaches are based on the single failure assumption. Under the condition of a single constellation, the common assumption is a single failure occurring at a time. The probability of multiple simultaneous failures cannot be neglected in the case of two constellations. In this case, the LSR RAIM approach does not provide sufficient integrity to the user. However, the simulations are run based on a single failure assumption.

The two RAIM approaches can be generalized to a multiple fault RAIM technique in which the protection level is computed by assuming that more than one measurement can be faulty at a given time. The only difference would be in the way the maximum slope is computed. Instead of searching for the satellite with the maximum slope, one must search for the linear combination of satellites that yields the maximum slope.

For LSR RAIM, the integrity risk is fully allocated to P_{md} , whereas the novel RAIM approach allocates of the integrity risk over two different threat cases.

For the novel RAIM, the main driver for HPL is the mapping factor from the vertical to the horizontal component. This mapping factor is dependent on the elevation mask that is used because low satellites drive the $S_{U,i}$ factor, which is the factor used to map the range error into the vertical component.

Results

This section summarizes the performance results of both the LSR RAIM by itself, and as supported by the novel RAIM approach. For the simulation a GPS constellation consisting of 24 satellites is assumed. In addition, the multi-constellation scenarios assume a Galileo constellation of 24 satellites. For the GPS only scenarios, the evaluation period is 1 day with a sampling rate of 30 s; for the GPS+Gal scenarios, an evaluation period of 10 days with a sampling rate of 300 s is assumed. An estimation accuracy of sea surface, $\sigma_{h, \text{sea surface}}$, of 1 m is assumed. The performance analyses were carried out by an adapted version of the MAAST tool (MAAST, 2014).

In the following analyses some integrity performance results are shown based on IMO requirements as well as for different masking angles.

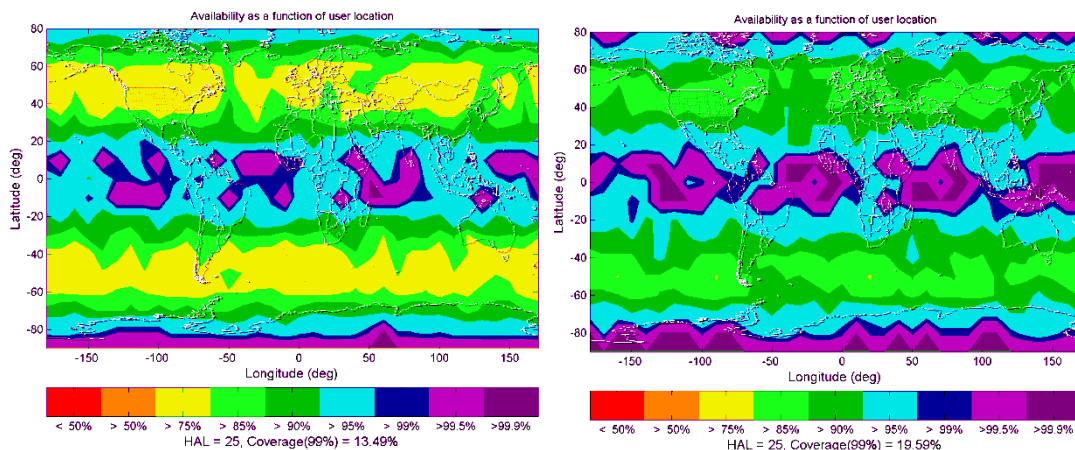


Figure 6. Availability of LSR RAIM (left) and novel RAIM (right) based on GPS only

The integrity performance of LSR RAIM (Figure 6, left) is slightly lower than that for the novel RAIM (Figure 6, right). Table 3 reveals an improvement of the availability performance using the novel RAIM for the GPS only scenario and an applied an elevation mask of 25°. For the dual-constellation scenario, the results show that the novel RAIM is able to provide sufficient integrity to be compliant with the requirements (99.5%). LSR RAIM is based on the single fault-only assumption, which is not sufficient to provide integrity at the required level of safety if the probability of having multiple simultaneous faults is not negligible.

Table 3. Availability results

	Availability [%]	
	LSR RAIM	Novel RAIM (25°)
GPS only	91.21	94.96
GPS+Gal	99.99	99.99

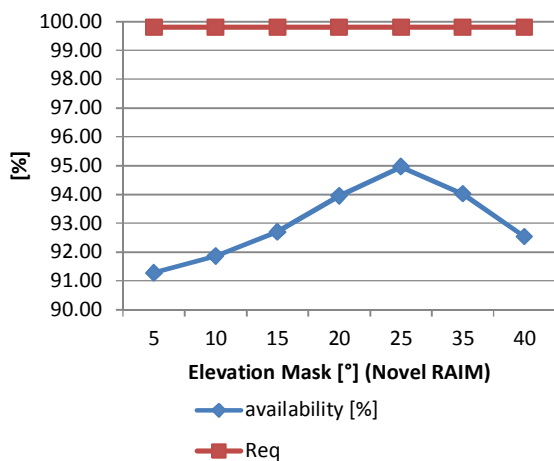


Figure 7. Elevation Dependency of MRAIM

The performance of the novel RAIM is strongly dependent on the elevation mask which is applied. This can be explained by the slope factor that is applied for the HPL computation. Satellites at lower elevation angles cause an increase in the slope factor. However, the maximum performance is achieved at a 25° elevation mask before the number of available satellites gets substantially low. Despite an increase of performance, the requirement cannot be met.

Conclusions

This paper proposes a novel RAIM scheme applicable to maritime users. It is assumed that the sea surface is approximated by a known height reference, namely the geoid. From that, an independent height reference can be derived which can be used

to cross-check the height information derived from GNSS. The possibility of performing fault detection is briefly discussed. However, it has been concluded that reliable fault detection can only be performed to a certain extent. Because the detection domain is represented by the vertical component, the contribution of a faulty satellite is more sensitive to the vertical component than to the horizontal component. Nevertheless, a way to derive horizontal protection levels is proposed. The performance of the LSR RAIM approach used for aviation has been assessed in the context of IMO requirements. The conclusion is that there is a benefit of using the novel RAIM approach relative to the LSR RAIM. For the dual-constellation case, the novel RAIM approach is able to provide sufficient integrity to satisfy the IMO requirements.

Acknowledgments

Special thanks to all my colleagues at Airbus and especially to Prof. Dr.-Ing. Dr. h.c. Bernhard Heck (KIT) for supporting me in this work.

References

- BROWN, G. (1992) A Baseline RAIM Scheme and a Note on the equivalence of the three RAIM methods. *Navigation*. 39. pp. 301–316.
- EGM08 (2008) *Spherical Harmonic Coefficients of EGM08*. [Online] Available from: <http://earthinfo.nga.mil/GandG/wgs84/gravitymod/egm2008>. [Accessed: 24th March 2015]
- Global Positioning System (2008) SPS Performance Standard for GPS.
- HAMMER, J. & DAVID, E. (2010) *Stochastic Analysis of ADS-B Integrity Requirements*. The MITRE Corporation, Digital Avionics Systems Conference (DASC), 2010 IEEE/AIAA 29th, 3–7 Oct. 2010.
- IMO (2002) IMO Resolution A.915(22) – Revised Maritime Policy and Requirements for a Future Global Navigation Satellite System (GNSS), 22.01.2002.
- ISSHIKI, H. (2008) *A New Method for Detection, Identification and Mitigation of Outliers in Receiver Autonomous Integrity Monitoring (RAIM)*. ION GNSS 21st International Technical Meeting of the Satellite Division, 16–19. September 2008, Savannah, GA.
- MAAST (2014) Matlab Algorithm Availability Simulation Tool [Online] Available from: <http://waas.stanford.edu/staff/maast/maast.html>. [Accessed: 22nd October 2014]
- Navipedia (2014) *European Space Agency*. [Online] Available from: <http://navipedia.org/>. [Accessed: 6th October 2014]
- RTCA/DO 229D (2006) Minimum Operational Performance Standards for Global Positioning Systems / Wide Area Augmentation System Airborne Equipment. RTCA, Inc., Washington D.C., USA.
- STURZA, M.A. (1988–1989) Navigation System Integrity Monitoring Using Redundant Measurements, *Navigation. Journal of the Institute of Navigation*. 35. 4. pp. 483–501.